Geophysical Research Letters

RESEARCH LETTER
10.1029/2020GL089300

Analyzing Internal Variability and Forced Response of Subdaily and Daily Extreme Precipitation Over Europe

R. R. Wood[1] and R. Ludwig[1]

[1]Department of Geography, LMU, Munich, Germany

Key Points:
- Subdaily extreme precipitation intensifies faster than daily extremes and mean precipitation
- On regional scales internal variability remains a dominant source of uncertainty until the end of the 21st century
- Widespread scaling rates of subdaily extremes above Clausius-Clapeyron over Northern and Eastern Europe

Supporting Information:
- Supporting Information S1

Correspondence to:
R. R. Wood,
raul.wood@lmu.de

Citation:
Wood, R. R., & Ludwig, R. (2020). Analyzing internal variability and forced response of subdaily and daily extreme precipitation over Europe. *Geophysical Research Letters*, *47*, e2020GL089300. https://doi.org/10.1029/2020GL089300

Received 11 JUN 2020
Accepted 4 AUG 2020
Accepted article online 10 AUG 2020

Abstract At regional to local scales internal variability is expected to be a dominant source of uncertainty in analyzing precipitation extremes and mean precipitation even far into the 21st century. A debated topic is whether a faster increase in subdaily precipitation extremes can be expected. Here we analyzed seasonal maximum precipitation in various time steps (3 hr, days, and 5 days) from a high-resolution 50-member large-ensemble (CRCM5-LE) and compared them to changes in mean precipitation over Europe. Our results show that the magnitude of change in extreme precipitation varies for season and duration. Subdaily extremes increase at higher rates than daily extremes and show higher scaling with temperature. Northern Europe shows widespread scaling above Clausius-Clapeyron of subdaily extremes in all seasons and for daily extremes in winter/spring. Scaling above Clausius-Clapeyron is also visible over Eastern Europe in winter/spring. For most regions and seasons the forced response emerges from the internal variability by midcentury.

Plain Language Summary The knowledge on how and why the intensity and frequency of extremes changes is critical to a resilient society. Our adaptive measures that are currently in place are based on observed extremes of the past. We know that observations are only one realization of a chaotic system and that the climate system is altered by natural variations, and anthropogenic contributions. Since we can only measure one realization of the world, we need climate models to investigate the influence of natural variability and anthropogenic factors. In this study we focus on the contribution of natural variability and the detection of regional patterns of changes in extreme precipitation. We used regional climate simulations, driven by multiple runs of global climate simulations under the same emission scenario, but with slight changes at the start of the simulation to imitate the butterfly effect of the climate system and simulate natural variability. We have found that natural variability plays a dominant role in the first half of the 21st century. But we have also found that subdaily extreme precipitation is increasing at a higher rate than daily extremes and that some of this change can be attributed to the warming of the atmosphere.

1. Introduction

Extreme precipitation events are becoming more likely under climate change due to atmospheric warming and the inherent alterations of the hydrological cycle (Allen & Ingram, 2002; Held & Soden, 2006; Wentz et al., 2007). Increasing intensities and frequencies of extreme events pose an imminent threat to humans, the economy, and the environment. On continental to global scales, models agree on the forced response (FR) of precipitation extremes (Fischer et al., 2014) and observations show increases in daily extreme precipitation (Alexander, 2016; Asadieh & Krakauer, 2015; Donat et al., 2016; Fischer & Knutti, 2016; Min et al., 2011; Westra et al., 2013) and subdaily extremes (Barbero et al., 2017; Guerreiro et al., 2018; Xiao et al., 2016) on a global scale.

There is currently a debate on whether subdaily precipitation extremes follow the Clausius-Clapeyron (CC) scaling or whether they increase at a higher rate. Based on observations and models, extreme precipitation is expected to increase with the availability of water vapor in the atmosphere, following the CC scaling of 6–7% per degree global warming. Mean precipitation on the other hand scales at a much lower rate of 1–3% per degree warming (Allen & Ingram, 2002; Held & Soden, 2006). Twice the CC scaling in hourly observations was first shown in Lenderink and van Meijgaard (2008) for stations in the Netherlands and was meanwhile shown for stations throughout the world (Westra et al., 2014, and references therein). This shift from CC to super-CC scaling (>7%/K) can be attributed to a shift from stratiform to convective precipitation (Berg

et al., 2013; Haerter & Berg, 2009; Molnar et al., 2015) and may also arise due to the physics of the clouds and the latent heat released during condensation, boosting the convection (Lenderink et al., 2017).

Climate models on global and regional scales project extreme precipitation to increase in the 21st century (Aalbers et al., 2018; Bao et al., 2017; Beniston et al., 2007; Boberg et al., 2010; Fischer et al., 2013; Fischer & Knutti, 2014; Martel et al., 2018, 2019; Pendergrass & Hartmann, 2014; Rajczak et al., 2013; Sillmann et al., 2013), which is attributable to human influences (Fischer & Knutti, 2015). Additionally, precipitation extremes are expected to undergo a shift in seasonality from summer to spring and autumn (Brönnimann et al., 2018; Marelle et al., 2018).

The internal variability (IV) of the climate system is an important source of uncertainty (Deser, Knutti, et al., 2012; Deser, Phillips, et al., 2012; Fischer et al., 2013, 2014; Hawkins & Sutton, 2009; Hegerl et al., 2004; Kendon et al., 2008; Lehner et al., 2020), especially on regional scales (Prein & Pendergrass, 2019). Over the middle and high latitudes IV might be in the same magnitude as the forced anthropogenic response (Deser, Knutti, et al., 2012; Deser, Phillips, et al., 2012). It originates from the coupled interaction of the land, atmosphere, oceans, and cryosphere (Deser et al., 2014), which is always present, even at longer timescales. Isolating the effects of IV from those of anthropogenic climate change requires ensembles of simulations from a given climate model that is subject to the identical external forcing (Deser et al., 2014). Kendon et al. (2008) and Kjellström et al. (2013) state that using large ensembles to Sample IV will lead to benefits in the ability to accurately project future changes in local precipitation extremes.

By using the large-ensemble approach the real FR can be analyzed. When using only one realization of a model the effects of IV are neglected and the analyzed realization only shows one possible change. This can also be true for small ensemble sizes in which the IV might be underrepresented and changes might be misinterpreted as significant (Milinski et al., 2019).

Several single-model initial-condition large ensembles (SMILEs) are now available which allow for the analysis of the IV and the real underlying FR of the model. There are several SMILEs available on the global scale (i.e., Fyfe et al., 2017; Kay et al., 2015; Maher et al., 2019). However, the magnitude, variability, and regional- to local-scale spatial patterns of climate variables are better represented in high-resolution RCMs (Chan et al., 2013; Giorgi et al., 2016; Kotlarski et al., 2014; Maraun et al., 2010; Prein et al., 2016). Several studies have shown that hourly precipitation is better represented in convection-permitting model (CPM) simulations (Kendon et al., 2017; Prein et al., 2015; Westra et al., 2014), and Berg et al. (2019) pointed out model deficiencies at hourly resolution in RCM simulations. However, due to their high computational cost the number of CPM simulations is still limited in time and spatial extent, which makes it difficult to study the effects of IV on local subdaily rainfall. Giorgi (2019) argues that due to the increased noise at CPM resolution we will require an ensemble of simulations. Therefore, large ensembles of RCMs are still the best estimate of IV on local to regional scales. The CRCM5 50-member large-ensemble (CRCM5-LE, Canadian Regional Climate Model Version 5) is the first Pan-European SMILE of high resolution (0.11°) (Leduc et al., 2019). Other regional large ensembles exist for Europe in coarser resolution (Addor & Fischer, 2015) or on a smaller domain (Aalbers et al., 2018).

In this study, the effects of climate change on the intensity change of seasonal and annual maximum 3-hourly (Rx3h), daily (Rx1d), 5-daily (Rx5d), and mean precipitation are analyzed alongside the influence of the IV. For this purpose, the simulations from the CRCM5-LE were analyzed to distinguish between the effect of climate change and natural variability. This study tries to answer these questions:

Is there a strong seasonal variability in the FR of maximum precipitation? When can we expect changes in extreme precipitation to robustly emerge from IV? Is the CC expression constraining scaling rates of precipitation extremes at subdaily and daily resolutions?

2. Data and Methods

2.1. Model Setup

The analysis of this paper is based on hourly precipitation data from the CRCM5-LE. The data originate from the first of its kind pan-European high-resolution initial-condition multimember dynamical downscaling experiment (Leduc et al., 2019) resulting in 50 equally likely transient (1950–2099) climate simulations from the same global climate (GCM) and regional climate model (RCM) combination. The multimember

initial-condition simulations from the Canadian Earth System Model version 2 Large-Ensemble (CanESM2-LE; Fyfe et al., 2017) were dynamically downscaled with the CRCM5 (v.3.3.3.1; Martynov et al., 2013; Šeparović et al., 2013) in a one-way nesting setup over Europe resulting in the 0.11° (approximately 12 km) resolution CRCM5-LE. All 50 CanESM2-LE simulations are driven with observed emissions (in CO_2 and non-CO_2 GHGs, aerosols, and land cover) during the historical period until 2005. For the subsequent period 2006–2099 all simulations were performed using the IPCC RCP8.5 scenario (Meinshausen et al., 2011). The differences among the single CRCM5 members are due to the small initial-condition perturbations in the driving CanESM2-LE and can be interpreted as the natural variability (in the following IV) of the climate system. At 0.11° resolution the CRCM5 model parameterizes deep convection following the approach of Kain and Fritsch (1990) and shallow convection is based on a transient version of Kuo (1965) scheme (Bélair et al., 2005).

2.2. Methods

For each member, season, and year the seasonal and annual maximum 3-hourly (Rx3h), daily (Rx1d), and 5-daily (Rx5d) precipitation was calculated, as well as seasonal (annual) mean precipitation. Seasonal maxima can be lower than annual maxima. The respective seasons are winter (DJF: December, January, and February), spring (MAM: March, April, and May), summer (JJA: June, July, and August), and fall (SON: September, October, and November). Changes in mean and extreme precipitation are differences in 30-year seasonal (annual) means compared to the reference period 1980–2009 calculated first for each member and afterward averaged over all 50 members. Figures 1–3 represent end of the century (2070–2099) changes, while Figure 4 shows transient changes.

The distribution of the 30-year mean values of the 50-members in the future was compared to the distribution in the reference period by applying a two-sided t test with unequal variances (p value: 0.01) to check for a significant change in the mean (Figure 1). The IV is determined as the standard deviation of the 50-member mean values (Figure 2) or relative changes (Figure 4).

There are several different ways to scale extreme precipitation with temperature by using the local or regional (dew point) temperature (Ban et al., 2015; Kendon et al., 2014, 2019) or binning with local temperature variations (X. Zhang, Zwiers, et al., 2017). Here we have scaled precipitation with the CRCM5 domain-averaged mean temperature change rather than using the local (grid cell) changes, because winterly and longer duration extremes can be expected to be influenced by remote moisture sources, which are insufficiently represented by local temperature. In Figure 3, the scaling rates are calculated as $\Delta P/\Delta T$ (%/K), where ΔP is, for example, the relative change in seasonal (annual) Rx3h and ΔT the change in mean seasonal (annual) surface temperature compared to 1980–2009.

Additionally, the time-of-emergence is marked, where the signals are for the first time exceeding the IV and remain above (Figure 4). Five regions of interest were analyzed (NEUR: Northern Europe, WEUR: Western Europe, CEUR: Central Europe, EEUR: Eastern Europe, and SEUR: Southern Europe; see Figure S1 in the supporting information).

For a general evaluation of the CRCM5-LE see Leduc et al. (2019), and for an evaluation of seasonal maximum precipitation and the timing of the annual maximum see the supporting information (Figures S10–S21).

3. Spatial Patterns of FR and IV

Annual maxima of subdaily precipitation are increasing throughout the European domain (EU) (Figure 1j), except for the Iberian Peninsula (IP, no change or decreasing). The FR of seasonal maxima (Figures 1f–1i) however reveals varying trends across seasons. While Rx3h is increasing throughout the EU in winter, and spring/fall showing similarity to the FR of annual maxima, the seasonal changes in summer are remarkably diverse. Over France and the Mediterranean Rx3h is strongly decreasing in summer, while CEUR, British Isles (BI) and NEUR showing prevailing increases.

Comparing these seasonal changes to changes of mean precipitation (Figure S4), then subdaily extremes show increasing trends over CEUR, BI, and southern Scandinavia, despite strong decreasing summerly mean precipitation over the majority of EU. These regional differences in FR can partly be explained by

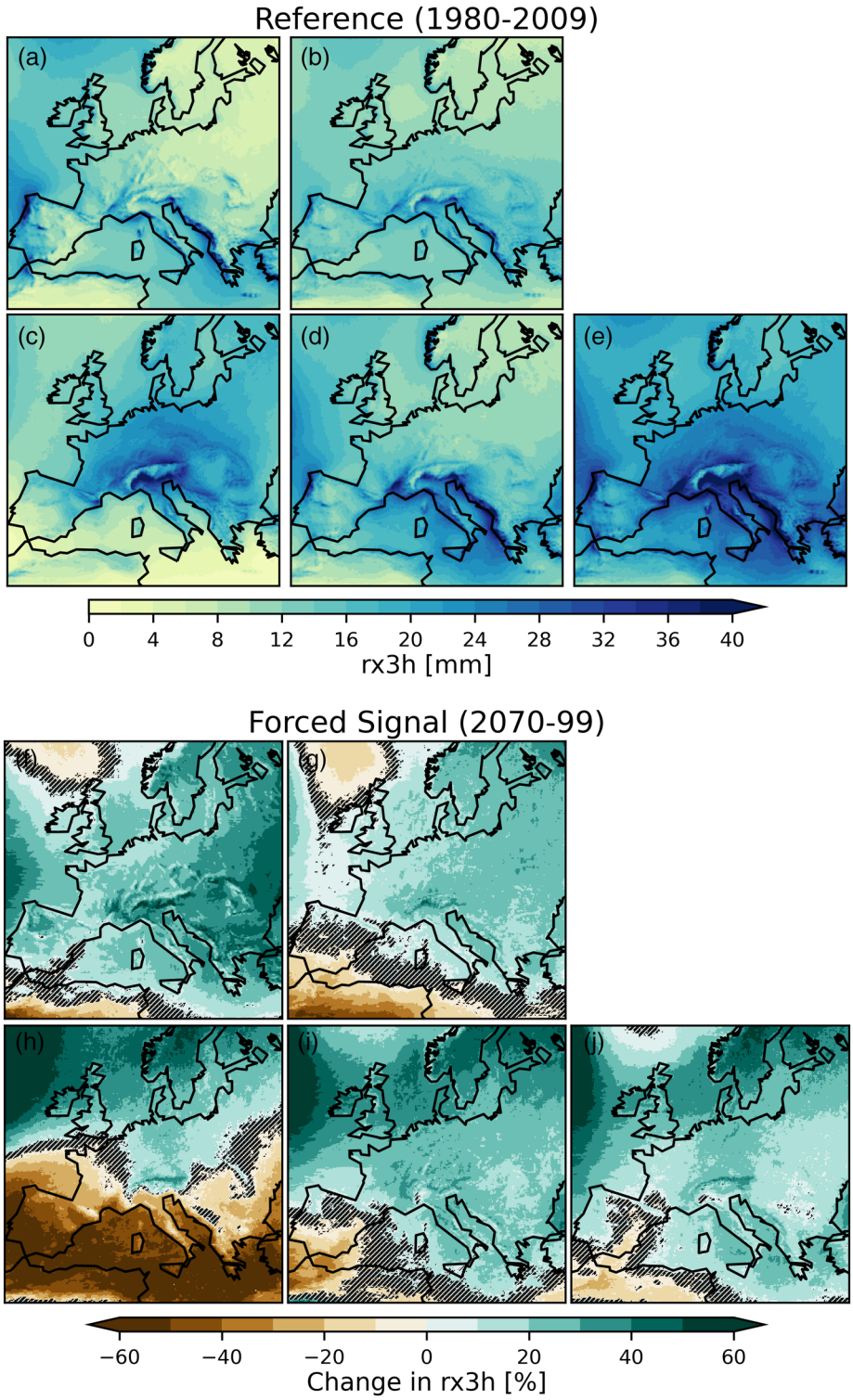

Figure 1. Spatial pattern of mean Rx3h in the reference period (1980–2009, a–e) and the 50-member mean forced signal in percent at the end of the century (2070–2099, f–j) for seasons winter (a, f), spring (b, g), summer (c, h), fall (d, i), and annual (e, j). Hatched areas in (f–j) indicate nonsignificant areas according to a two-sided *t* test with unequal variances (*p* value: 0.01).

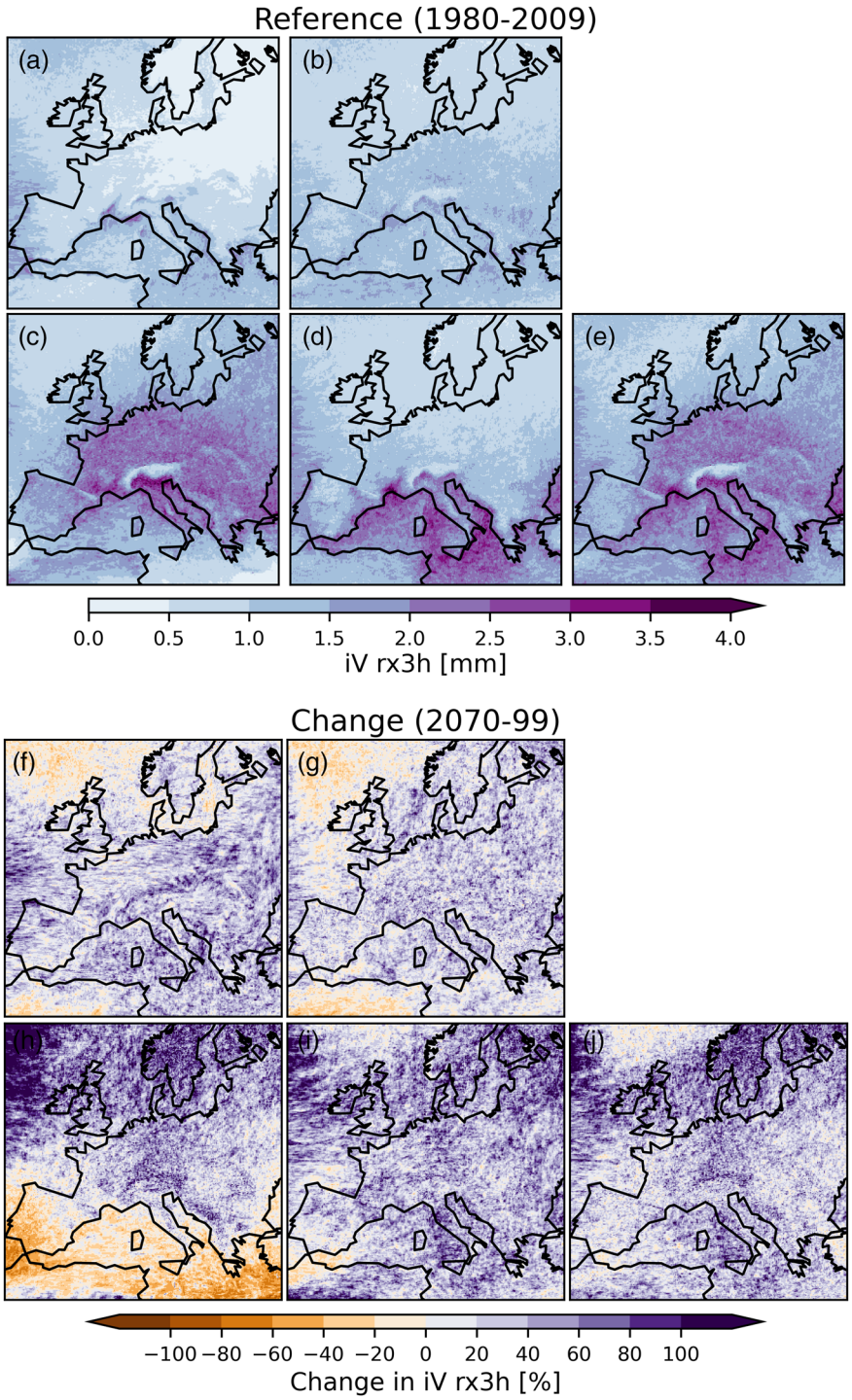

Figure 2. Internal variability of Rx3h in the reference period (1980–2009, a–e) and relative changes by 2070–99 (f–j) for seasons winter (a, f), spring (b, g), summer(c, h), fall (d, i), and annual (e, j).

the continued availability of moisture for the formation of convection. The Bowen Ratio (BR), which is the ratio between sensible and latent heat flux, indicates the continued dominance of latent heat over the regions with increasing Rx3h in summer (Figure S5). The regions with decreasing Rx3h on the other hand show a dramatic increase in BR, indicating an increase in sensible heat. Especially over the Mediterranean, the decreasing mean precipitation in the preceding season amplifies the lack of moisture from surface.

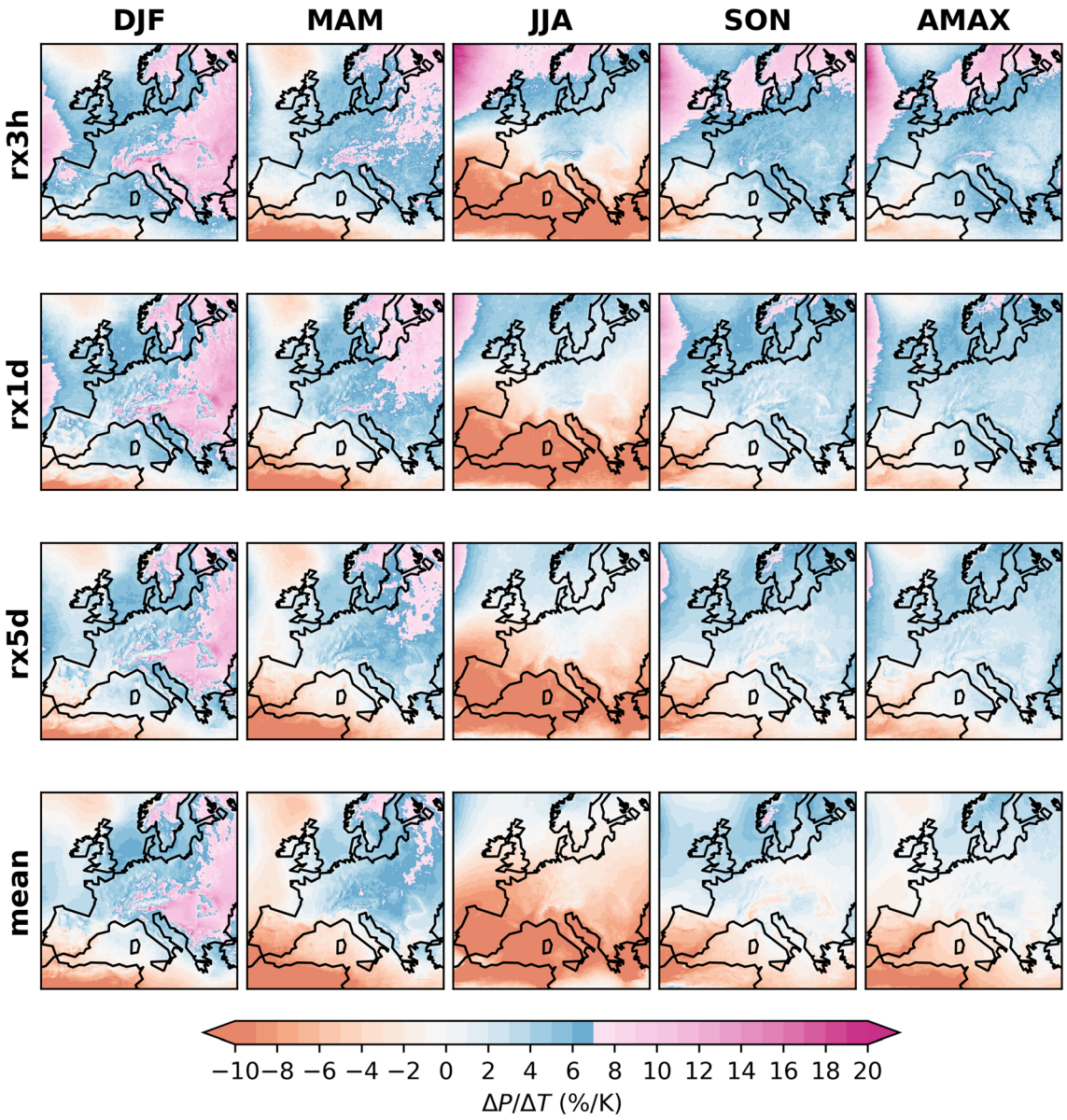

Figure 3. Precipitation scaling with domain-average temperature change by 2070–2099 compared to 1980–2009. Columns indicate seasons/annual; rows indicate extreme indices (Rx3h, Rx1d, and Rx5d) and mean precipitation (mean). Areas with a negative scaling are shown in red colors; scaling above the Clausius-Clapeyron scaling (>7%/K) is shown in magenta colors.

The patterns for the FR of Rx1d (Figures S2f–S2j) are similar to Rx3h, however showing overall lower changes for seasonal as well as annual maxima. Rx1d can originate from shorter duration rainfall bursts, hence the similarity to subdaily maxima. Rx5d originate from stratiform precipitation rather than convective precipitation and therefore show closer resemblance to the FR of mean precipitation (Figures S3f–S3j for Rx5d and Figures S4f–S4j for mean precipitation). In general, longer duration extremes increase at a lower rate than subdaily extremes.

The IV of Rx3h is in general highest in summer and lowest in winter (Figures 2a–2d), which is attributable to the role of convection in summer. However, in high-elevation regions (Alps and Pyrenees) the variability in summer is remarkable lower than their surroundings, which might indicate a lack of convection. In general, the IV of Rx3h is homogeneous over large areas of the domain only showing topographic features in summer. The IV of Rx1d, Rx5d, and mean precipitation show higher values along large topographic features (Figures S6a–S6e, S7a–S7e, and S8a–S8e).

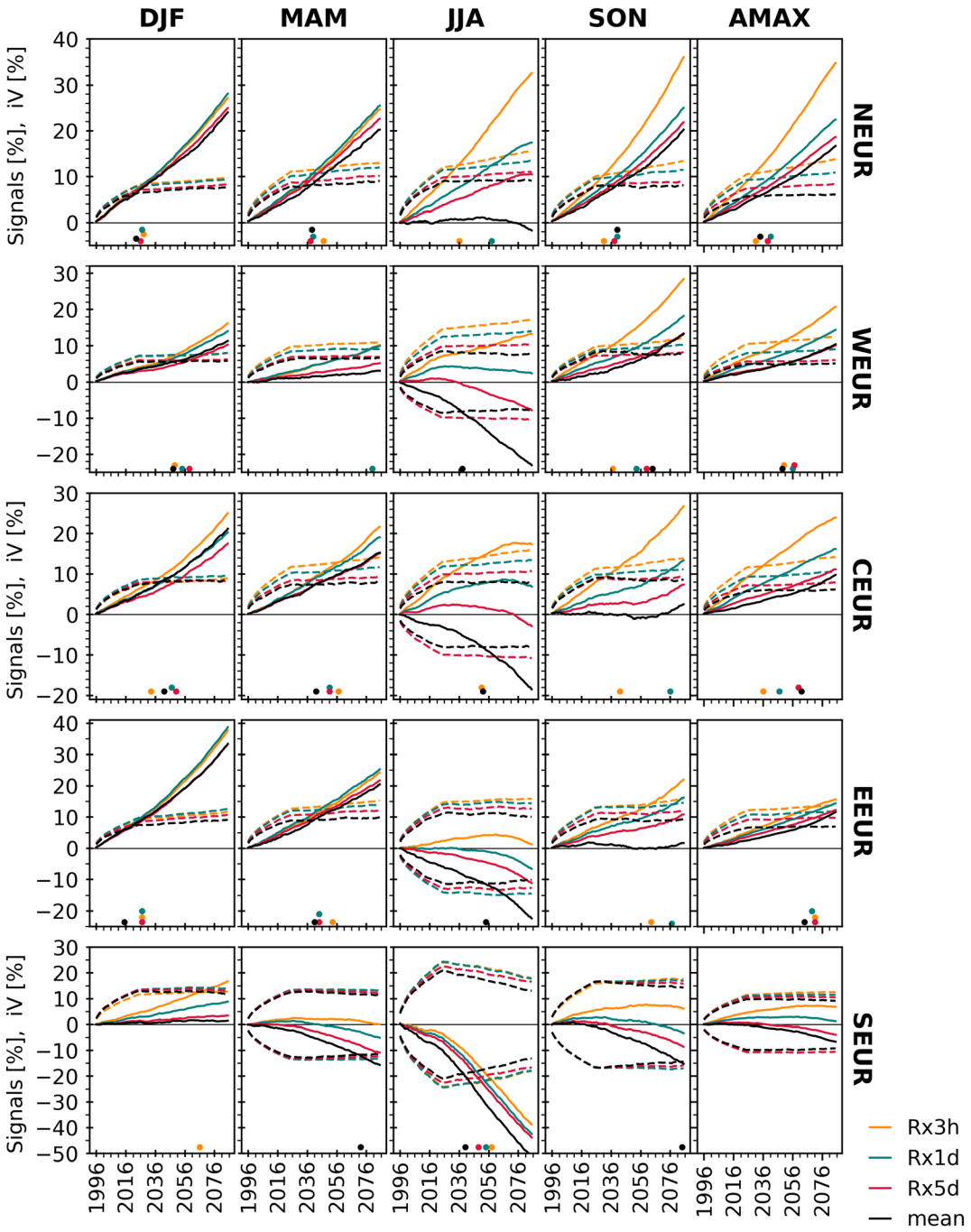

Figure 4. Transient 30-year moving window of forced response and internal variability. Solid lines: ensemble-mean relative changes, dashed lines: internal variability (standard deviation of the 50-member relative changes). If signals show negative values, the internal variability is shown as positive and negative. Columns: seasons and annual; rows: regions. Points indicate the time-of-emergence where signal/noise remains above 1.

The changes of IV by the end of the century reveal an increase in variability for seasonal and annual Rx3h (Figures 2f–2j) throughout the EU. NEUR show strong relative changes in IV in summer, fall, and annual maxima, which indicates the increasing role of convection. In contrast the variability over the IP is decreasing in summer for Rx3h as well as all other indices (Figures S6h, S7h, and S8h), which implies, together with the strong decrease in FR, the increasing lack of precipitation over the IP and Mediterranean Sea.

In general, the changes of IV for Rx1d, Rx5d, and mean precipitation are regionally more diverse than for Rx3h, showing small areas throughout the domain with increases and decreases in all seasons. This emphasizes the role of IV as a source of uncertainty on regional scales.

4. Scaling With Mean Temperature Change

Scaling changes with temperature allows for a first look at whether changes can be attributed to thermodynamics or if it is rather likely to be influenced by dynamic changes. Figure 3 shows CC or super-CC scaling (>7%/K) for Rx3h over NEUR throughout all seasons and for annual maxima, which implies thermodynamics having a dominant role. Other regions also indicate super-CC scaling for Rx3h mainly in winter and partly in spring over EEUR, the Balkan Peninsula, Northern Italy, southern part of CEUR, or Northwestern IP. In summer and in the annual maxima, parts of the Alps show super-CC scaling for Rx3h, which might be connected to an increase of convective events over high alpine elevations as shown in Giorgi et al. (2016). Longer duration extremes show generally considerably less areas with super-CC scaling, and mainly only in winter and partly in spring. This can also be seen in Figure S9.

The large proportion of land areas without CC-scaling or negative scaling indicates that the changes are mainly driven by other effects than thermodynamics. In some recent studies (Kröner et al., 2017; Pfahl et al., 2017) it is shown that other factors may have stronger contributions than thermodynamics. Pfahl et al. (2017) argue that the negative changes in extreme precipitation can be related to decreases in the vertical velocity, which can even offset the influence of thermodynamic change. The changes of regional dynamics might partly be attributed to a northward shift of present day pattern of vertical velocity, which can be related to a general expansion of the Hadley cells (Kröner et al., 2017; Pfahl et al., 2017). As a result of the extension of the Hadley cell, SEUR would become more strongly affected by subsidence, which would lead to reduced convection (Kröner et al., 2017). Brogli et al. (2019) argue that Hadley cells only have a small influence on European climate change and rather propose a change in lapse rates and meridional change as important factors. Also, changes in cyclone intensities can play a role as shown for the Mediterranean (Pfahl et al., 2017; Zappa et al., 2015). Other factors that can contribute to a drying are the land-ocean warming contrast and soil-moisture feedbacks (Kröner et al., 2017).

5. Transient Changes of Extreme Precipitation and Emergence From IV

Looking at the evolution of the FR and IV (Figure 4), there is a clear tendency in all regions and all seasons that shorter extremes show stronger signals for both intensity and IV. In general, the Rx3h is the upper bound of change and mean precipitation the lower bound. The Rx3h and Rx1d show a very similar FR in several regions, mainly in winter or spring. In summer, the Rx3h exceeds by far the other indices showing a large discrepancy between the change in mean precipitation and Rx3h. The change in mean precipitation and Rx3h are counter directional in all regions except NEUR. Thus, this implies that different processes govern the response of the hydrological cycle. Tang et al. (2018) explain the drying of the south and wetting of north, by showing an enhanced sea-level-pressure pattern (similar to NAO-AO), which can divert the jet stream and storm tracks northward reducing precipitation in the Mediterranean and increasing precipitation in NEUR in summer.

Apart from the summer signals, smooth linear trends are visible tending to accelerate toward the end of the century. WEUR shows a strong trend for Rx3h within the first 10 years followed by a period of reduced increase and acceleration toward the end again. This altered near future behavior is also visible for Rx1d, which is followed by a slow decrease in summer; Rx5d in summer shows no trend at first, then decreases. CEUR and EEUR show linear trends for summer until around 2060 with a followed flattening in CEUR and a reversal in EEUR. These hooked shape trends might indicate that land-atmosphere feedbacks undergo a considerable change under global warming. This might indicate that the moisture availability rather than the storage capacity of the atmosphere constrains extreme precipitation (Berg et al., 2009; Drobinski et al., 2016; Hardwick Jones et al., 2010) and therefore only seen in summer, where mean precipitation is largely decreasing.

Madsen et al. (2014) conclude an increase in daily extreme precipitation based on observations for several European areas, confirming the findings of the projected future changes in daily extreme precipitation in

this study: over the United Kingdom in winter, spring, and autumn; over Germany and western Czech Republic in winter; over French Mediterranean regions; Belgium and Northeastern Italy.

In Figure 4, the IV is defined as the standard deviation of the 50-member relative changes. The IV is increasing for about three decades before stabilizing at around 10–20% in SEUR and 5–15% in other regions. It shows the importance of IV on shorter timescales and after stabilizing an emergence of robust signals depends on the intensity of the FR. The uncertainty from IV plays an important role on regional scales until midcentury, as also shown by Lehner et al. (2020). The decrease in IV toward the end of the century over SEUR in summer can be explained by approaching zero precipitation, which leads to a compression of the standard deviation.

The information about the FR and the IV can be used to assess whether a signal is strong and attributable to climate change or whether the change is still clouded by the uncertainty that lies within the range of IV. The time when the signal leaves the band of IV (a signal-to-noise ratio greater than 1) is referred to as time-of-emergence. The Rx3h emerges in almost all seasons and regions from the IV before the middle of the century.

Only where the FR is small emergence is either reached later or no emergence before the end of the century is reached. Where the FR of Rx3h is smaller or like Rx1d, the FR of subdaily extremes emerges later than the daily FR due to smaller IV in Rx1d. Otherwise, subdaily extremes generally emerge before daily extremes. For seasonal maxima in winter as well as for annual maxima all indices show an emergence before the end of the century, except in SEUR. Here, only in summer all indices agree on an emergence before midcentury. In general, the signals of all indices emerge earlier in winter than in summer, which can be attributed to higher values of IV in summer. Indices emerging in the second half of the century or not emerging at all highlight the importance of IV as a dominant source of uncertainty on regional scales late into the 21st century.

6. Conclusion and Discussion

In this study we have analyzed seasonal and annual maximum precipitation for various temporal resolutions (3-hr, days, and 5 days) from the CRCM5-LE under the RCP8.5 scenario.

Is the CC expression constraining scaling rates of precipitation extremes at subdaily and daily resolutions? We show that subdaily extremes (Rx3h) exhibit stronger increases and higher CC-scaling than daily extremes and mean precipitation. These findings are consistent with other studies (e.g., W. Zhang, Villarini, et al., 2017). While regions such as NEUR and EEUR exhibit precipitation extremes with super-CC scaling (>7%/K), which might indicate that changes are mainly driven by thermodynamics, other areas such as France or SEUR seem to be strongly influenced by dynamic changes (e.g., a change in storm tracks or altered latent heat flux induced by reduced soil moisture). In these regions the alterations of the IV could also be triggered by dynamic changes.

Is there a strong seasonal variability in the FR of maximum precipitation? The trends of Rx3h can differ considerably from one season to the other. While NEUR and WEUR show even higher trends for summer, SEUR shows decreasing trends in summer compared to increases (winter) or no change.

When can we expect changes in extreme precipitation to robustly emerge from IV? Despite the dominant source of uncertainty induced by the IV, robust signals can be detected within the 21st century on regional scales. For almost all indices and seasons a time-of-emergence before midcentury can be projected. The Rx3h tends to emerge earlier than daily indices or mean precipitation, as well as an earlier emergence in winter over summer, which is also suggested by Kendon et al. (2018). However, especially in areas with small signals the IV remains a dominant source of uncertainty even until the end of the century. Also, Prein and Pendergrass (2019) and Lehner et al. (2020) argue that on regional scales IV will remain a dominant source of uncertainty.

Since the signals predominantly emerge before 2050, they are likely to be independent of the RCP scenario. The rate of extreme precipitation change scaled with temperature does not substantially vary across RCP scenarios (Berg et al., 2019; Pendergrass et al., 2015) until the midcentury, and even late in the 21st century there is still a considerable overlap for RCP4.5 and RCP8.5 results (Sanderson et al., 2018). Also, Lehner

et al. (2020) show that scenario uncertainty becomes relevant after 2050. Therefore, we can have confidence in the sign of extreme precipitation change, the higher scaling of subdaily extremes versus longer duration extremes, and the evolution of the IV.

Comparing our results with the only other high-resolution large-ensemble study over Western Europe (Aalbers et al., 2018) indicates a strong coherence of the regional pattern of mean and extreme precipitation, which implies that other regional SMILEs agree in the increase in extreme precipitation as well as their spatial patterns. However, as shown by Berg et al. (2019) RCMs show model deficiencies for hourly summer precipitation due the parametrization of convection that may alter the magnitude of change. It would be important to extend this study to CPM simulations to study the impact of convection parametrization on the results shown for subdaily extremes. Innocenti et al. (2019) showed for North America that the CRCM5-LE can reproduce the annual and diurnal cycle of annual maximum daily and subdaily precipitation and that they are comparable to a 4 km WRF simulation. For four smaller European regions Hodnebrog et al. (2019) compared the CRCM5-LE to 3 km WRF simulations and show that the WRF CPM shows smaller increases of summerly Rx1h but that both show a stronger intensification of subdaily extremes compared to daily extremes or mean precipitation and that IV is a dominant source of uncertainty.

On the regional scale more high-resolution large ensembles are needed to comprehensively analyze the robustness of regional patterns and to narrow down the individual sources of uncertainties that arise from model deficiencies, emission scenarios, and IV.

Data Availability Statement

The CRCM5-LE precipitation data are available to the scientific community online (http://www.climex-project.org).

Acknowledgments
The CRCM5-LE was created within the ClimEx project, which was funded by the Bavarian State Ministry for the Environment and Consumer Protection. Computations of the CRCM5-LE were made on the SuperMUC supercomputer at Leibniz Supercomputing Centre of the Bavarian Academy of Sciences and Humanities. We acknowledge Environment and Climate Change Canada for providing the CanESM2-LE driving data.

References

Aalbers, E. E., Lenderink, G., van Meijgaard, E., & van den Hurk, B. J. J. M. (2018). Local-scale changes in mean and heavy precipitation in Western Europe, climate change or internal variability? *Climate Dynamics*, *50*(11–12), 4745–4766. https://doi.org/10.1007/s00382-017-3901-9

Addor, N., & Fischer, E. M. (2015). The influence of natural variability and interpolation errors on bias characterization in RCM simulations. *Journal of Geophysical Research: Atmospheres*, *120*, 10,180–10,195. https://doi.org/10.1002/2014JD022824

Alexander, L. V. (2016). Global observed long-term changes in temperature and precipitation extremes: A review of progress and limitations in IPCC assessments and beyond. *Weather and Climate Extremes*, *11*, 4–16. https://doi.org/10.1016/j.wace.2015.10.007

Allen, M. R., & Ingram, W. J. (2002). Constraints on future changes in climate and the hydrologic cycle. *Nature*, *419*(6903), 228–232. https://doi.org/10.1038/nature01092

Asadieh, B., & Krakauer, N. Y. (2015). Global trends in extreme precipitation: Climate models versus observations. *Hydrology and Earth System Sciences*, *19*(2), 877–891. https://doi.org/10.5194/hess-19-877-2015

Ban, N., Schmidli, J., & Schär, C. (2015). Heavy precipitation in a changing climate: Does short-term summer precipitation increase faster? *Geophysical Research Letters*, *42*, 1165–1172. https://doi.org/10.1002/2014GL062588

Bao, J., Sherwood, S. C., Alexander, L. V., & Evans, J. P. (2017). Future increases in extreme precipitation exceed observed scaling rates. *Nature Climate Change*, *7*(2), 128–132. https://doi.org/10.1038/nclimate3201

Barbero, R., Fowler, H. J., Lenderink, G., & Blenkinsop, S. (2017). Is the intensification of precipitation extremes with global warming better detected at hourly than daily resolutions? *Geophysical Research Letters*, *44*, 974–983. https://doi.org/10.1002/2016GL071917

Bélair, S., Mailhot, J., Girard, C., & Vaillancourt, P. (2005). Boundary layer and shallow cumulus clouds in a medium-range forecast of a large-scale weather system. *Monthly Weather Review*, *133*(7), 1938–1960. https://doi.org/10.1175/MWR2958.1

Beniston, M., Stephenson, D. B., Christensen, O. B., Ferro, C. A. T., Frei, C., Goyette, S., et al. (2007). Future extreme events in European climate: An exploration of regional climate model projections. *Climatic Change*, *81*(S1), 71–95. https://doi.org/10.1007/s10584-006-9226-z

Berg, P., Christensen, O. B., Klehmet, K., Lenderink, G., Olsson, J., Teichmann, C., & Yang, W. (2019). Summertime precipitation extremes in a EURO-CORDEX 0.11° ensemble at an hourly resolution. *Natural Hazards and Earth System Sciences*, *19*(4), 957–971. https://doi.org/10.5194/nhess-19-957-2019

Berg, P., Haerter, J. O., Thejll, P., Piani, C., Hagemann, S., & Christensen, J. H. (2009). Seasonal characteristics of the relationship between daily precipitation intensity and surface temperature. *Journal of Geophysical Research*, *114*, D18102. https://doi.org/10.1029/2009JD012008

Berg, P., Moseley, C.r., & Haerter, J. O. (2013). Strong increase in convective precipitation in response to higher temperatures. *Nature Geoscience*, *6*(3), 181–185. https://doi.org/10.1038/ngeo1731

Boberg, F., Berg, P., Thejll, P., Gutowski, W. J., & Christensen, J. H. (2010). Improved confidence in climate change projections of precipitation further evaluated using daily statistics from ENSEMBLES models. *Climate Dynamics*, *35*(7–8), 1509–1520. https://doi.org/10.1007/s00382-009-0683-8

Brogli, R., Kröner, N., Sørland, S. L., Lüthi, D., & Schär, C. (2019). The role of Hadley circulation and lapse-rate changes for the future European summer climate. *Journal of Climate*, *32*(2), 385–404. https://doi.org/10.1175/JCLI-D-18-0431.1

Brönnimann, S., Rajczak, J., Fischer, E. M., Raible, C. C., Rohrer, M., & Schär, C. (2018). Changing seasonality of moderate and extreme precipitation events in the Alps. *Natural Hazards and Earth System Sciences*, *18*(7), 2047–2056. https://doi.org/10.5194/nhess-18-2047-2018

Chan, S. C., Kendon, E. J., Fowler, H. J., Blenkinsop, S., Ferro, C. A. T., & Stephenson, D. B. (2013). Does increasing the spatial resolution of a regional climate model improve the simulated daily precipitation? *Climate Dynamics*, *41*(5–6), 1475–1495. https://doi.org/10.1007/s00382-012-1568-9

Deser, C., Knutti, R., Solomon, S., & Phillips, A. S. (2012). Communication of the role of natural variability in future North American climate. *Nature Climate Change*, *2*(11), 775–779. https://doi.org/10.1038/nclimate1562

Deser, C., Phillips, A., Bourdette, V., & Teng, H. (2012). Uncertainty in climate change projections: The role of internal variability. *Climate Dynamics*, *38*(3–4), 527–546. https://doi.org/10.1007/s00382-010-0977-x

Deser, C., Phillips, A. S., Alexander, M. A., & Smoliak, B. V. (2014). Projecting North American climate over the next 50 years: Uncertainty due to internal variability. *Journal of Climate*, *27*(6), 2271–2296. https://doi.org/10.1175/JCLI-D-13-00451.1

Donat, M. G., Alexander, L. V., Herold, N., & Dittus, A. J. (2016). Temperature and precipitation extremes in century-long gridded observations, reanalyses, and atmospheric model simulations. *Journal of Geophysical Research: Atmospheres*, *121*, 11,174–11,189. https://doi.org/10.1002/2016JD025480

Drobinski, P., Alonzo, B., Bastin, S., Silva, N. D., & Muller, C. (2016). Scaling of precipitation extremes with temperature in the French Mediterranean region: What explains the hook shape? *Journal of Geophysical Research: Atmospheres*, *121*, 3100–3119. https://doi.org/10.1002/2015JD023497

Fischer, E. M., Beyerle, U., & Knutti, R. (2013). Robust spatially aggregated projections of climate extremes. *Nature Climate Change*, *3*(12), 1033–1038. https://doi.org/10.1038/nclimate2051

Fischer, E. M., & Knutti, R. (2014). Detection of spatially aggregated changes in temperature and precipitation extremes. *Geophysical Research Letters*, *41*, 547–554. https://doi.org/10.1002/2013GL058499

Fischer, E. M., & Knutti, R. (2015). Anthropogenic contribution to global occurrence of heavy-precipitation and high-temperature extremes. *Nature Climate Change*, *5*(6), 560–564. https://doi.org/10.1038/nclimate2617

Fischer, E. M., & Knutti, R. (2016). Observed heavy precipitation increase confirms theory and early models. *Nature Climate Change*, *6*(11), 986–991. https://doi.org/10.1038/nclimate3110

Fischer, E. M., Sedláček, J., Hawkins, E., & Knutti, R. (2014). Models agree on forced response pattern of precipitation and temperature extremes. *Geophysical Research Letters*, *41*, 8554–8562. https://doi.org/10.1002/2014GL062018

Fyfe, J. C., Derksen, C., Mudryk, L., Flato, G. M., Santer, B. D., Swart, N. C., et al. (2017). Large near-term projected snowpack loss over the western United States. *Nature Communications*, *8*, 14,996. https://doi.org/10.1038/ncomms14996

Giorgi, F. (2019). Thirty years of regional climate modeling: Where are we and where are we going next? *Journal of Geophysical Research: Atmospheres*, *124*, 5696–5723. https://doi.org/10.1029/2018JD030094

Giorgi, F., Torma, C., Coppola, E., Ban, N., Schär, C., & Somot, S. (2016). Enhanced summer convective rainfall at Alpine high elevations in response to climate warming. *Nature Geoscience*, *9*(8), 584–589. https://doi.org/10.1038/ngeo2761

Guerreiro, S. B., Fowler, H. J., Barbero, R., Westra, S., Lenderink, G., Blenkinsop, S., et al. (2018). Detection of continental-scale intensification of hourly rainfall extremes. *Nature Climate Change*, *8*(9), 803–807. https://doi.org/10.1038/s41558-018-0245-3

Haerter, J. O., & Berg, P. (2009). Unexpected rise in extreme precipitation caused by a shift in rain type? *Nature Geoscience*, *2*(6), 372–373. https://doi.org/10.1038/ngeo523

Hardwick Jones, R., Westra, S., & Sharma, A. (2010). Observed relationships between extreme sub-daily precipitation, surface temperature, and relative humidity. *Geophysical Research Letters*, *37*, L22805. https://doi.org/10.1029/2010GL045081

Hawkins, E., & Sutton, R. (2009). The potential to narrow uncertainty in regional climate predictions. *Bulletin of the American Meteorological Society*, *90*(8), 1095–1108. https://doi.org/10.1175/2009BAMS2607.1

Hegerl, G. C., Zwiers, F. W., Stott, P. A., & Kharin, V. v. (2004). Detectability of anthropogenic changes in annual temperature and precipitation extremes. *Journal of Climate*, *17*(19), 3683–3700. https://doi.org/10.1175/1520-0442(2004)017<3683:DOACIA>2.0.CO;2

Held, I. M., & Soden, B. J. (2006). Robust responses of the hydrological cycle to global warming. *Journal of Climate*, *19*(21), 5686–5699. https://doi.org/10.1175/JCLI3990.1

Hodnebrog, Ø., Marelle, L., Alterskjær, K., Wood, R. R., Ludwig, R., Fischer, E. M., et al. (2019). Intensification of summer precipitation with shorter time-scales in Europe. *Environmental Research Letters*, *14*(12), 124,050. https://doi.org/10.1088/1748-9326/ab549c

Innocenti, S., Mailhot, A., Frigon, A., Cannon, A. J., & Leduc, M. (2019). Observed and simulated precipitation over northeastern North America: How do daily and sub-daily extremes scale in space and time? *Journal of Climate. Advance online publication.*, *32*(24), 8563–8582. https://doi.org/10.1175/JCLI-D-19-0021.1

Kain, J. S., & Fritsch, J. M. (1990). A one-dimensional entraining/detraining plume model and its application in convective parameterization. *Journal of the Atmospheric Sciences*, *47*(23), 2784–2802. https://doi.org/10.1175/1520-0469(1990)047<2784:AODEPM>2.0.CO;2

Kay, J. E., Deser, C., Phillips, A., Mai, A., Hannay, C., Strand, G., et al. (2015). The Community Earth System Model (CESM) large ensemble project: A community resource for studying climate change in the presence of internal climate variability. *Bulletin of the American Meteorological Society*, *96*(8), 1333–1349. https://doi.org/10.1175/BAMS-D-13-00255.1

Kendon, E. J., Ban, N., Roberts, N. M., Fowler, H. J., Roberts, M. J., Chan, S. C., et al. (2017). Do convection-permitting regional climate models improve projections of future precipitation change? *Bulletin of the American Meteorological Society*, *98*(1), 79–93. https://doi.org/10.1175/BAMS-D-15-0004.1

Kendon, E. J., Blenkinsop, S., & Fowler, H. J. (2018). When will we detect changes in short-duration precipitation extremes? *Journal of Climate*, *31*(7), 2945–2964. https://doi.org/10.1175/JCLI-D-17-0435.1

Kendon, E. J., Roberts, N. M., Fowler, H. J., Roberts, M. J., Chan, S. C., & Senior, C. A. (2014). Heavier summer downpours with climate change revealed by weather forecast resolution model. *Nature Climate Change*, *4*(7), 570–576. https://doi.org/10.1038/nclimate2258

Kendon, E. J., Rowell, D. P., Jones, R. G., & Buonomo, E. (2008). Robustness of future changes in local precipitation extremes. *Journal of Climate*, *21*(17), 4280–4297. https://doi.org/10.1175/2008JCLI2082.1

Kendon, E. J., Stratton, R. A., Tucker, S., Marsham, J. H., Berthou, S., Rowell, D. P., & Senior, C. A. (2019). Enhanced future changes in wet and dry extremes over Africa at convection-permitting scale. *Nature Communications*, *10*(1), 1794. https://doi.org/10.1038/s41467-019-09776-9

Kjellström, E., Thejll, P., Rummukainen, M., Christensen, J. H., Boberg, F., Christensen, O. B., & Fox Maule, C. (2013). Emerging regional climate change signals for Europe under varying large-scale circulation conditions. *Climate Research*, *56*(2), 103–119. https://doi.org/10.3354/cr01146

Kotlarski, S., Keuler, K., Christensen, O. B., Colette, A., Déqué, M., Gobiet, A., et al. (2014). Regional climate modeling on European scales: A joint standard evaluation of the EURO-CORDEX RCM ensemble. *Geoscientific Model Development*, *7*(4), 1297–1333. https://doi.org/10.5194/gmd-7-1297-2014

Kröner, N., Kotlarski, S., Fischer, E. M., Lüthi, D., Zubler, E., & Schär, C. (2017). Separating climate change signals into thermodynamic, lapse-rate and circulation effects: Theory and application to the European summer climate. *Climate Dynamics*, *48*(9–10), 3425–3440. https://doi.org/10.1007/s00382-016-3276-3

Kuo, H. L. (1965). On formation and intensification of tropical cyclones through latent heat release by cumulus convection. *Journal of the Atmospheric Sciences*, *22*(1), 40–63. https://doi.org/10.1175/1520-0469(1965)022<0040:OFAIOT>2.0.CO;2

Leduc, M., Mailhot, A., Frigon, A., Martel, J.-L., Ludwig, R., Brietzke, G. B., et al. (2019). ClimEx project: A 50-member ensemble of climate change projections at 12-km resolution over Europe and northeastern North America with the Canadian Regional Climate Model (CRCM5). *Journal of Applied Meteorology and Climatology*, *58*(4), 663–693. https://doi.org/10.1175/JAMC-D-18-0021.1

Lehner, F., Deser, C., Maher, N., Marotzke, J., Fischer, E. M., Brunner, L., et al. (2020). Partitioning climate projection uncertainty with multiple large ensembles and CMIP5/6. *Earth System Dynamics*, *11*(2), 491–508. https://doi.org/10.5194/esd-11-491-2020

Lenderink, G., Barbero, R., Loriaux, J. M., & Fowler, H. J. (2017). Super-Clausius–Clapeyron scaling of extreme hourly convective precipitation and its relation to large-scale atmospheric conditions. *Journal of Climate*, *30*(15), 6037–6052. https://doi.org/10.1175/JCLI-D-16-0808.1

Lenderink, G., & van Meijgaard, E. (2008). Increase in hourly precipitation extremes beyond expectations from temperature changes. *Nature Geoscience*, *1*(8), 511–514. https://doi.org/10.1038/ngeo262

Madsen, H., Lawrence, D., Lang, M., Martinkova, M., & Kjeldsen, T. R. (2014). Review of trend analysis and climate change projections of extreme precipitation and floods in Europe. *Journal of Hydrology*, *519*, 3634–3650. https://doi.org/10.1016/j.jhydrol.2014.11.003

Maher, N., Milinski, S., Suarez-Gutierrez, L., Botzet, M., Dobrynin, M., Kornblueh, L., et al. (2019). The max Planck institute grand ensemble—Enabling the exploration of climate system variability. *Journal of Advances in Modeling Earth Systems*, *11*, 2050–2069. https://doi.org/10.1029/2019MS001639

Maraun, D., Wetterhall, F., Ireson, A. M., Chandler, R. E., Kendon, E. J., Widmann, M., et al. (2010). Precipitation downscaling under climate change: Recent developments to bridge the gap between dynamical models and the end user. *Reviews of Geophysics*, *48*, RG3003. https://doi.org/10.1029/2009RG000314

Marelle, L., Myhre, G., Hodnebrog, Ø., Sillmann, J., & Samset, B. H. (2018). The changing seasonality of extreme daily precipitation. *Geophysical Research Letters*, *45*, 11,352–11,360. https://doi.org/10.1029/2018GL079567

Martel, J.-L., Mailhot, A., & Brissette, F. (2019). Global and regional projected changes in 100-year sub-daily, daily and multi-day precipitation extremes estimated from three large ensembles of climate simulation. *Journal of Climate. Advance online publication*, *33*(3), 1089–1103. https://doi.org/10.1175/JCLI-D-18-0764.1

Martel, J.-L., Mailhot, A., Brissette, F., & Caya, D. (2018). Role of natural climate variability in the detection of anthropogenic climate change signal for mean and extreme precipitation at local and regional scales. *Journal of Climate*, *31*(11), 4241–4263. https://doi.org/10.1175/JCLI-D-17-0282.1

Martynov, A., Laprise, R., Sushama, L., Winger, K., Šeparović, L., & Dugas, B. (2013). Reanalysis-driven climate simulation over CORDEX North America domain using the Canadian Regional Climate Model, version 5: Model performance evaluation. *Climate Dynamics*, *41*(11–12), 2973–3005. https://doi.org/10.1007/s00382-013-1778-9

Meinshausen, M., Smith, S. J., Calvin, K., Daniel, J. S., Kainuma, M. L. T., Lamarque, J.-F., et al. (2011). The RCP greenhouse gas concentrations and their extensions from 1765 to 2300. *Climatic Change*, *109*(1–2), 213–241. https://doi.org/10.1007/s10584-011-0156-z

Milinski, S., Maher, N., & Olonscheck, D. (2019). How large does a large ensemble need to be? *Earth Syst. Dynam. Discuss. Advance online publication*. https://doi.org/10.5194/esd-2019-70

Min, S.-K., Zhang, X., Zwiers, F. W., & Hegerl, G. C. (2011). Human contribution to more-intense precipitation extremes. *Nature*, *470*(7334), 378–381. https://doi.org/10.1038/nature09763

Molnar, P., Fatichi, S., Gaál, L., Szolgay, J., & Burlando, P. (2015). Storm type effects on super Clausius–Clapeyron scaling of intense rainstorm properties with air temperature. *Hydrology and Earth System Sciences*, *19*(4), 1753–1766. https://doi.org/10.5194/hess-19-1753-2015

Pendergrass, A. G., & Hartmann, D. L. (2014). Changes in the distribution of rain frequency and intensity in response to global warming. *Journal of Climate*, *27*(22), 8372–8383. https://doi.org/10.1175/JCLI-D-14-00183.1

Pendergrass, A. G., Lehner, F., Sanderson, B. M., & Xu, Y. (2015). Does extreme precipitation intensity depend on the emissions scenario? *Geophysical Research Letters*, *42*, 8767–8774. https://doi.org/10.1002/2015GL065854

Pfahl, S., O'Gorman, P. A., & Fischer, E. M. (2017). Understanding the regional pattern of projected future changes in extreme precipitation. *Nature Climate Change*, *7*(6), 423–427. https://doi.org/10.1038/nclimate3287

Prein, A. F., Gobiet, A., Truhetz, H., Keuler, K., Goergen, K., Teichmann, C., et al. (2016). Precipitation in the EURO-CORDEX 0.11° and 0.44° simulations: High resolution, high benefits? *Climate Dynamics*, *46*(1–2), 383–412. https://doi.org/10.1007/s00382-015-2589-y

Prein, A. F., Langhans, W., Fosser, G., Ferrone, A., Ban, N., Goergen, K., et al. (2015). A review on regional convection-permitting climate modeling: Demonstrations, prospects, and challenges. *Reviews of Geophysics*, *53*, 323–361. https://doi.org/10.1002/2014RG000475

Prein, A. F., & Pendergrass, A. G. (2019). Can we constrain uncertainty in hydrologic cycle projections? *Geophysical Research Letters*, *46*, 3911–3916. https://doi.org/10.1029/2018GL081529

Rajczak, J., Pall, P., & Schär, C. (2013). Projections of extreme precipitation events in regional climate simulations for Europe and the Alpine Region. *Journal of Geophysical Research: Atmospheres*, *118*, 3610–3626. https://doi.org/10.1002/jgrd.50297

Sanderson, B. M., Oleson, K. W., Strand, W. G., Lehner, F., & O'Neill, B. C. (2018). A new ensemble of GCM simulations to assess avoided impacts in a climate mitigation scenario. *Climatic Change*, *146*(3–4), 303–318. https://doi.org/10.1007/s10584-015-1567-z

Šeparović, L., Alexandru, A., Laprise, R., Martynov, A., Sushama, L., Winger, K., et al. (2013). Present climate and climate change over North America as simulated by the fifth-generation Canadian regional climate model. *Climate Dynamics*, *41*(11–12), 3167–3201. https://doi.org/10.1007/s00382-013-1737-5

Sillmann, J., Kharin, V. V., Zwiers, F. W., Zhang, X., & Bronaugh, D. (2013). Climate extremes indices in the CMIP5 multimodel ensemble: Part 2. Future climate projections. *Journal of Geophysical Research: Atmospheres*, *118*, 2473–2493. https://doi.org/10.1002/jgrd.50188

Tang, T., Shindell, D., Samset, B. H., Boucher, O., Forster, P. M., Hodnebrog, Ø., et al. (2018). Dynamical response of Mediterranean precipitation to greenhouse gases and aerosols. *Atmospheric Chemistry and Physics*, *18*(11), 8439–8452. https://doi.org/10.5194/acp-18-8439-2018

Wentz, F. J., Ricciardulli, L., Hilburn, K., & Mears, C. (2007). How much more rain will global warming bring? *Science (New York, N.Y.)*, *317*(5835), 233–235. https://doi.org/10.1126/science.1140746

Westra, S., Alexander, L. V., & Zwiers, F. W. (2013). Global increasing trends in annual maximum daily precipitation. *Journal of Climate*, *26*(11), 3904–3918. https://doi.org/10.1175/JCLI-D-12-00502.1

Westra, S., Fowler, H. J., Evans, J. P., Alexander, L. V., Berg, P., Johnson, F., et al. (2014). Future changes to the intensity and frequency of short-duration extreme rainfall. *Reviews of Geophysics*, *52*, 522–555. https://doi.org/10.1002/2014RG000464

Xiao, C., Wu, P., Zhang, L., & Song, L. (2016). Robust increase in extreme summer rainfall intensity during the past four decades observed in China. *Scientific Reports*, *6*, 38,506. https://doi.org/10.1038/srep38506

Zappa, G., Hawcroft, M. K., Shaffrey, L., Black, E., & Brayshaw, D. J. (2015). Extratropical cyclones and the projected decline of winter Mediterranean precipitation in the CMIP5 models. *Climate Dynamics*, *45*(7–8), 1727–1738. https://doi.org/10.1007/s00382-014-2426-8

Zhang, W., Villarini, G., Scoccimarro, E., & Vecchi, G. A. (2017). Stronger influences of increased CO_2 on subdaily precipitation extremes than at the daily scale. *Geophysical Research Letters*, *44*, 7464–7471. https://doi.org/10.1002/2017GL074024

Zhang, X., Zwiers, F. W., Li, G., Wan, H., & Cannon, A. J. (2017). Complexity in estimating past and future extreme short-duration rainfall. *Nature Geoscience*, *10*(4), 255–259. https://doi.org/10.1038/ngeo2911